AN EXPERIMENTAL INVESTIGATION OF WIND LOAD ON TALL BUILDINGS WITH HEXAGONAL CROSS-SECTION

Kaniz Ronak Sultana [(1)], Dr. Amalesh Chandra Mandal [(2)], Bhuiyan Shameem Mahmood Ebna Hai [(3)]

1. M.Sc in ME, Department of Mechanical Engineering, BUET, E-mail: kaniz.buet@engineer.com

2. Faculty of Mechanical Engineering Department, BUET, E-mail: amalesh@me.buet.ac.bd

3. Faculty of Mechanical Engineering Department, MIST, E-mail: shameem.me@mist.edu.bd

ABSTRACT

An experimental investigation of surface static pressure distributions on hexagonal cylinder was conducted. The study was performed on both the single cylinder and the group consisting of two cylinders, one in the upstream and another in the downstream side. The test was conducted in an open circuit wind tunnel at a Reynolds number of 4.13 x 104 based on the face width of the cylinder across the flow direction in a uniform flow of velocity 13.2 m/s. The study was done on the single cylinder at various angles of attack from 00 to 500 at a step of 100. The surface pressure distributions were measured with the help of an inclined manometer. Then the group of two cylinders was taken into consideration for the study and the surface static pressures were measured for various inter-spacing of 1D, 2D, 3D, 4D, 6D and 8 D, D being the width of the cylinder across the flow direction. In each case the wind velocity was kept constant at 13.2 m/s. The pressure coefficients were calculated from the measured values of the surface static pressure distributions on the cylinder. Then the drag and lift coefficients were obtained from the pressure coefficients by the numerical integration method. It was observed that the drag coefficients become remarkably smaller compared to those for a sharp-edged square cylinder. It was also observed that at various angles of attack, the values of the lift coefficients were insignificant compared to those for a sharp-edged square cylinder. It can be further concluded that the hexagonal cylinder produces significantly low values of drag and lift forces and they approach to those of the cylinder with circular cross-section.

Keywords: Reynolds Number, Lift, Drag, Pressure coefficient, Lift and drag coefficient.

1.0 INTRODUCTION

The subject of wind load on buildings and structures is not a new one. In the 17th century, Galileo and Newton have considered the effect of wind loading on buildings, but during that period, it did not gain popularity. The effect of wind loading on buildings and structures has been considered for design purposes since late in the 19th century; but starting from that time up to about 1950, the studies in this field have not been considered seriously. Buildings and their components are to be designed to withstand the code-specified wind loads. Calculating wind loads is important in the design of wind force-resisting system, including structural members, components, and cladding against shear, sliding, overturning, and uplift actions.

In recent years, much emphasis has been given on "The Study of Wind Effect on Buildings and Structures" in the different corners of the world. Even researchers in Bangladesh have taken much interest in this field. Till now, little attention has been paid to the flow over the bluff bodies like square cylinders, rectangular cylinders, hexagonal cylinders etc. and some information is available concerning the flow over them in staggered condition, although this is a problem of considerable practical significance. With the progressing world, engineering problems regarding wind loads around a group of skyscrapers, chimneys, towers and the flow induced vibration of tubes in heat exchangers, bridges, oil rigs or marine structures need detailed investigation of flow patterns and aerodynamic characteristics. Arising from the increasing practical importance of bluff body aerodynamics, over the past few decades sufficient effort has been given in research works concerning laboratory simulations, full-scale measurements and more recently numerical calculations and theoretical predictions for flows over bodies of wide variety of shapes. A number of failures of bridges, transmission towers, buildings and housings over the last one hundred years prompted researchers to do research work in this field. The study of wind effect was first limited to loading on buildings and structures only, possibly

because of its most dramatic effects are seen in their collapses. In mid-sixties researchers started the study of less dramatic, but equally important environmental aspects of flow of wind around buildings. These include the effects on pedestrians, weathering, rain penetration, ventilation, heat loss, wind noise and air pollution etc. The pioneer researcher in this field is Lawson T V [8] of the University of Bristol. A number of works of the environmental aspects of wind was being studied at the Building Research Establishment at Garson and the University of Bristol, UK.

It is true that researchers from all over the world have contributed greatly to the knowledge of flow over bluff bodies as published by Mchuri F G et al [10] but the major part of the reported works are of fundamental nature involving the flow over single body of different profiles. Most of the researchers have conducted works either on single cylinder with circular, square or rectangular section etc. or in a group with them for various flow parameters. However, the flow over hexagonal cylinders has not been studied extensively especially in-groups to date, although this is a problem of practical significance. It is believed that the study on the cylinder with hexagonal section will contribute to find the wind load on the single and group of hexagonal buildings and the results will be useful to the relevant engineers and architects.

2.0 EXPERIMENTAL SETUP AND PROCEDURE

The experimental investigation to find wind load on the hexagonal cylinder was conducted at the exit end of a wind tunnel. The schematic diagram of the experimental setup of the present investigation has been shown in Figure 1. Open circuit subsonic type wind tunnel was used to develop the required flow and the cylinders were positioned at the exit end of the wind tunnel in the downstream side. The tunnel is 5.93 meter long with a test section of 460 x 480 mm cross-section. In order to make the flow uniform a honeycomb is fixed near the end of the wind tunnel. The wind tunnel consists of a bell-shaped converging mouth entry. A digital anemometer is used in each of these tests to measure the wind velocity. It was the low speed wind tunnel having the maximum wind velocity of 14 m/s in the test section. In the tunnel test section, the measured velocity distribution was uniform.

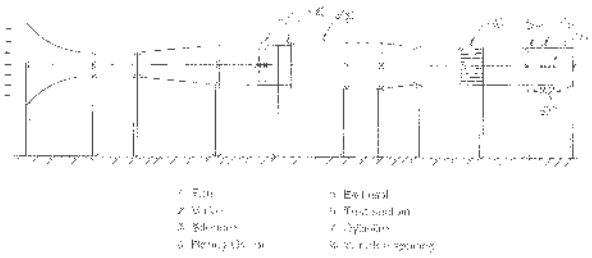

Figure 1: Schematic Diagram of Wind Tunnel

In each case of the tests, wind velocity is measured directly with the help of a digital anemometer. The flow velocity in the test section was maintained at 13.2m/s approximately. The measured velocity distribution was almost uniform across the tunnel test section in the upstream side of the test models. The pattern of the flow velocity is shown in Figure 2 in the non-dimensional form.

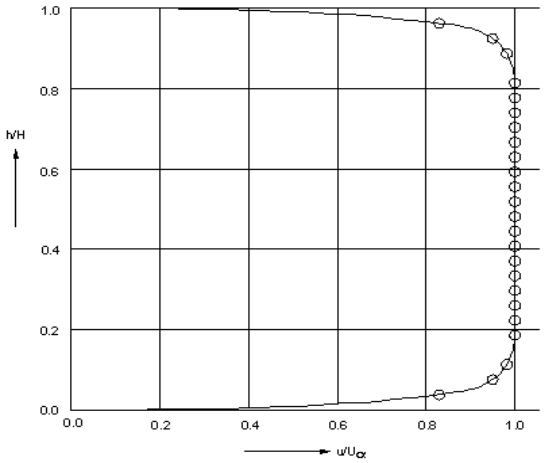

Figure 2: Velocity Distribution at Upstream Side of Model Cylinder

In reality the test was done at the exit end of the wind tunnel in the open air as shown in Figure 1. In order to fix the cylinder a steel frame was fabricated, the top floor of which was at the same level of the wind tunnel at the exit end. Two side walls were attached to the steel frame at the two sides by the help of nut and bolt. The distance between the extended side walls was equal to the distance of the side walls of the wind tunnel exit end. This distance of between the side walls was 460 mm. The length of the test section was 400 mm. There was no cover plate at the top and bottom of the extended test section.

The cylinders were fixed with the extended sidewalls. The sidewalls were made of plywood. In one side, the model cylinder was fastened with the side wall using nut and bolt. The bolt was

fixed with one end of the cylinder. Through the other end of the cylinder, the plastic tubes were taken out in order to connect them with the inclined multi-manometer. This end was supported in the groove of the sidewall of the extended portion, compatible with the hexagonal end of the cylinder. The capillary tube made of copper was used to make the tapping on the sides of the hexagonal model cylinders. These copper tubes were connected with the plastic tubes. The cylinder was leveled and then fixed very carefully so that its top and bottom sides were parallel to the flow direction.

There was a provision for rotation of the test cylinder at various angles to obtain the wind load at different angles of attack The Reynolds number was 00000 based on the projected width of the cylinder across the flow direction. Since the top and bottom of the extended part of the wind tunnel was open; as such no correction for blockage was done in the analysis. The test cylinders were placed very close to the end of the wind tunnel so that the approach velocity on the test cylinders was approximately identical as that in the exit end of the wind tunnel.

The provision was also kept in the extended wall to fix the two hexagonal cylinders side by side along the flow direction. These two cylinders were the part of the group. There was also a scope to change the interspacing between the cylinders. The interspacing between the two cylinders was varied at 1D, 2D, 3D, 4D, 6D and 8D. With a view to achieving this, several groups were made on the side walls of the test section. When the test was conducted, the unnecessary groves were sealed. The cylinders were fixed at one end by the help of bolt and nut and the other ends were fixed in groove. Through the grooves the plastic tubes were taken out and connected with the inclined multi-manometer as in the single cylinder. During fixing the cylinders, it was carefully checked whether the top and bottom sides of the cylinders were parallel to the free stream velocity direction. The rear cylinder was fixed behind the front cylinder along the flow direction. Leveling of the test cylinder was always checked by a standard spirit level.

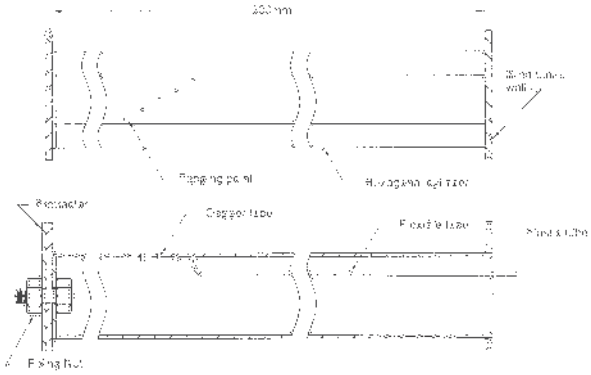

Figure 3: Taping Positions Shown on Longitudinal Section of Cylinder

In Figure 3 the taping positions on the longitudinal section of the cylinder is shown. There were six tapings on each face of the cylinder. The distance between the consecutive taping points was equal (Δd) as shown in the figure. However, the location of the corner taping was at a distance of ½ Δd. Each taping was identified by a numerical number from 1 to 30 as can be seen from the figure.

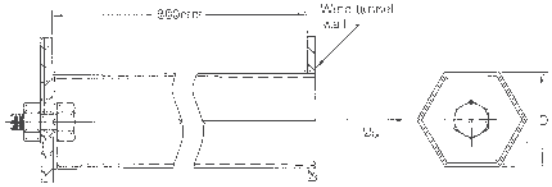

Figure 4: Tunnel Test Section Showing Position of Single Cylinder

In Figure 4 the position of the single cylinder at zero angle of attack is shown in the wind tunnel test section. In this position the top and bottom faces of the hexagonal cylinder were parallel to the flow direction. In this position the width of the cylinder was 50 mm in a direction perpendicular to the flow. Based on this width the Reynolds number was calculated. The surface static pressure distributions on six faces of the cylinder were measured in this position. Then the cylinder was rotated at an angle of 10^0 and the static pressure distributions on each face of the cylinder were measured again. The same test procedure was repeated to measure the surface static pressure distributions of the cylinders with angles of attack of 20^0, 30^0, 40^0 and 50^0.

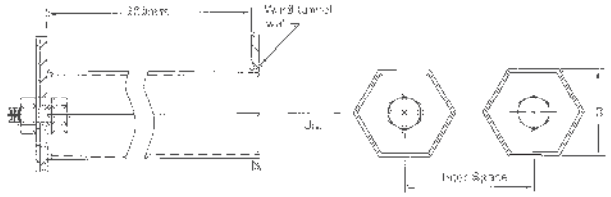

Figure 5: Tunnel Test Section Showing Position of Group of Cylinders

In Figure 5 the position of the group of cylinders at zero angle of attack is shown in the wind tunnel test section. The inter-spacing between the front cylinder and the rear cylinder was taken as 1D i.e. 50mm. Then static surface pressure distributions were measured on the six faces of the front and the rear cylinders. Keeping everything identical the inter-spacing was changed to 2D and the experiment was repeated. Next, the inter-spacing was varied to 4D, 6D, and 8D and in each case the static pressure distributions on both the front and the rear cylinders were taken. All the measurements were taken at zero angle of attack only.

All the data are hereby presented in terms of non-dimensional coefficients. The coefficients of lift, drag and total force were obtained by numerical integration method.

Pressure co-efficient is defined as,

$$C_P = \frac{\Delta P}{\frac{1}{2}\rho U_\infty^2} \quad \text{----------(1)}$$

Drag co-efficient is defined as,

$$C_D = \frac{F_D}{\frac{1}{2}\rho A U_\infty^2} \quad \text{----------(2)}$$

Lift co-efficient is defined as,

$$C_L = \frac{F_L}{\frac{1}{2}\rho A U_\infty^2} \quad \text{----------(3)}$$

The effect of wind on the structure as a whole is determined by the combined action of external and internal pressures acting upon it. In all cases, the calculated wind loads act normal to the surface to which they apply.

3.0RESULTS AND DISCUSSION

3.1 Distribution of Pressure Coefficients

The cross-section of the single hexagonal model cylinder with 30 numbers of tapings, 5 numbers on each surface of the cylinder at an angle of attack has been shown in Figure 6. The six surfaces have been identified with S_1, S_2, S_3, S_4, S_5 and S_6. Pressure coefficient for each taping point has been determined from the measured surface static pressure.

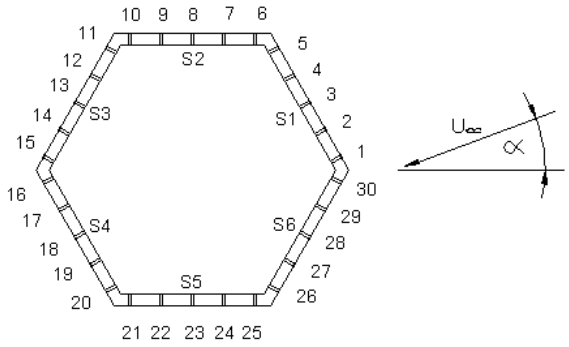

Figure 6: Taping Positions Shown on Cross-Section of Cylinder

In Figures 7, the distributions of static pressure coefficients for angles of attack of 0^0 to 50^0 with a step of 10^0 have been presented respectively. While in Figure 7, the distributions of pressure coefficients for all angles of attack have been shown for relative comparison and C_p-distribution on the surfaces S_3 to S_5 is almost uniform.

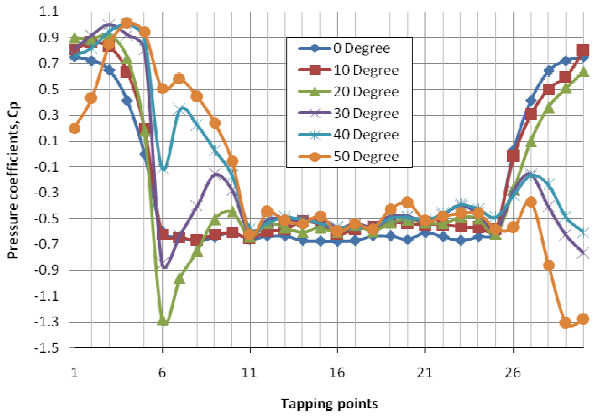

Figure 7: Distribution of Pressure Coefficients at Different Angles of Attack.

3.2 Variation of Drag Coefficient

Variation of drag coefficient at various angles of attack on single hexagonal cylinder is shown in Figure 8. The drag coefficient at different angles of attack on a single square cylinder at uniform flow obtained by Mandal A C [9] is also presented in this figure for comparison. It can be noticed from this figure that there is significant drop in the drag coefficient values for the hexagonal cylinder in comparison to that of the square cylinder and the values approaches to that of the circular cylinder. It is seen from this figure that at zero angle of attack, the drag coefficient is about 0.95 and at all other angles of attack, the values are close to 0.8 except at angle of attack of 10^0, where the value is about 0.5. The values of the drag

coefficient at various angles of attack for the hexagonal cylinder can be explained from the C_p-distribution curves.

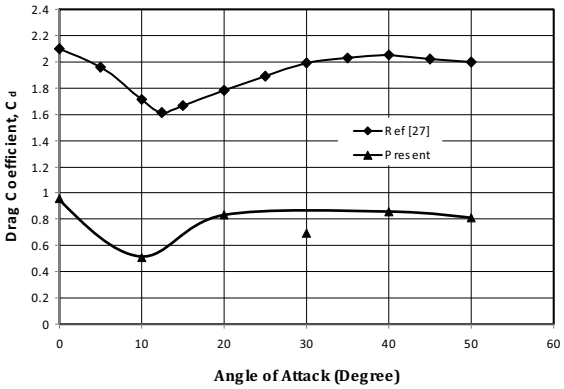

Figure 8: Variation of Drag Coefficient at Various Angles of attack on Single Cylinder

3.3 Variation of Lift Coefficient

In Figure 9 the variation of lift coefficient at various angles of attack on single hexagonal cylinder is shown. The lift coefficient at different angles of attack on a square cylinder at uniform flow obtained by Mandal A C [9] is also presented in this figure for comparison. it can be noticed from this figure that the variation of the lift coefficient on the single hexagonal cylinder is not appreciable; they are close to zero value except at angles of attack of 10^0 and 50^0, where some insignificant values are observed. For the single square cylinder the variation of lift coefficient with angle of attack is remarkable. The values of the lift coefficients for the single hexagonal cylinder can be explained from the C_p-distribution curves.

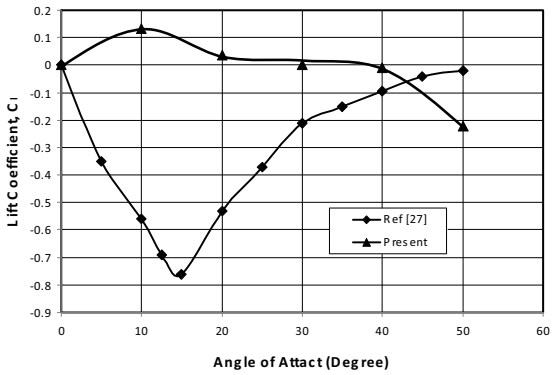

Figure 9: Variation of Lift Coefficient at Various Angles of Attack on Single Cylinder

3.4 Group of Cylinders

In this section discussion in regard to the results of the group consisting of two hexagonal cylinders will be done. In Figure 10, the group of cylinders is shown at zero angle of attack. One cylinder is positioned in the upstream side designated as the front cylinder and another one is positioned in the downstream side designated as the rear cylinder. Both of them are placed along the flow direction. The inter-spacing between them will only be varied at 1D, 2D, 3D, 4D, 5D and 6D keeping the angle of attack constant. Taping points are shown along the cross-section on the six surfaces S_1, S_2, S_3, S_4, S_5 and S_6 of the cylinder, where the surface static pressures were measured.

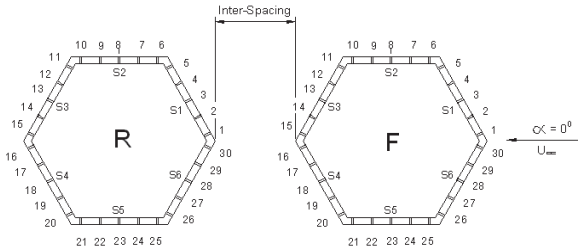

Figure 10: Flow over Cylinders in Group at Zero Angle of Attack

3.4.1 Distribution of Pressure Coefficients on Front Cylinder

The C_p-distribution on the front cylinder of the group at the inter-spacing of 1D, 2D, 3D, 4D, 5D and 6D is shown in Figure 11. It can be seen from this figure that the C_p-distribution is more or less identical to that of the single cylinder at zero angle of attack. That is, there is little effect on the C_p-distribution of the front cylinder due the presence of the rear cylinder. However, the positive C_p values have been increased slightly on the surfaces S_1 and S_6 compared to those on the single cylinder. There is more or less uniform distribution of C_p on the surfaces S_2 to S_5.

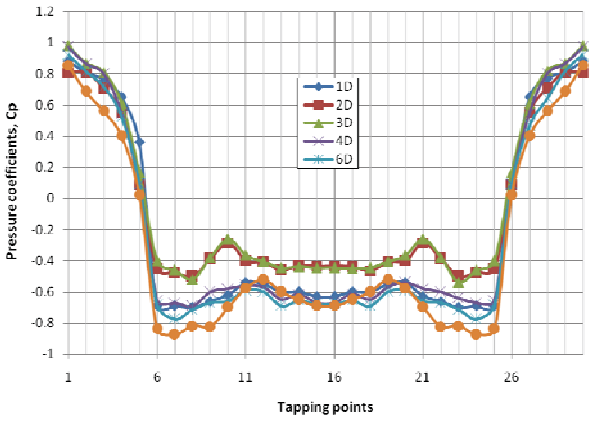

Figure 11: Distribution of Pressure Coefficients at zero angles of attack with different interspacing on Front Cylinder.

3.4.2 Distribution of Pressure Coefficient on Rear Cylinder

The C_p-distribution on the rear cylinder at the inter-spacing of 1D, 2D, 3D, 4D, 5D and 6D is shown in Figure 12. It can be observed from this figure that there is remarkable effect on C_p-distribution due the presence of the front cylinder. In the upstream side on the surfaces S_1 and S_6 there is high suction, while on the surfaces S_2 to S_5, suction reduces appreciably in comparison to that of either front cylinder with different inter-spacing at zero angle of attack. The front surfaces S_1 and S_6 of the rear cylinder fall in the suction zone created by the front cylinder and there is no stagnation point here.

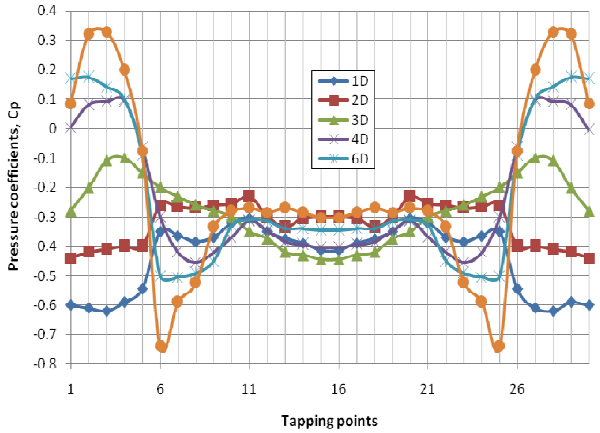

Figure 12: Distribution of Pressure Coefficients at zero angles of attack with different interspacing on rear cylinder.

3.5 Variation of Drag Coefficient on Front and Rear Cylinder

The variation of drag coefficients on the front and rear cylinders of the group at different inter-spacing at zero degree angle of attack has been presented in Figure 13. It can be seen from this figure that the drag coefficient on the front cylinder is about unity. Except at the inter-spacing of 1D, at all other inter-spacing the drag coefficients on the front cylinder of the group are higher than that on the single hexagonal cylinder. That is, due to the interference of the flow by the rear cylinder, there has been increase of the drag values on the front cylinder of the group at all inter-spacing except at the inter-spacing of 1D in comparison to the single hexagonal cylinder.
However, there has been remarkable drop in the drag value on the rear cylinder of the group. From Figure 13 it is observed that at some inter-spacing between 2D and 3 D, the drag coefficient on the rear cylinder is zero. At the higher inter-spacing the drag coefficients are positive and at lower inter-spacing they are negative. The drag coefficient on the rear cylinder of the group drops mainly because the front surfaces S_1 and S_6 of the rear cylinder fall within the suction side generated by the front cylinder of the group.

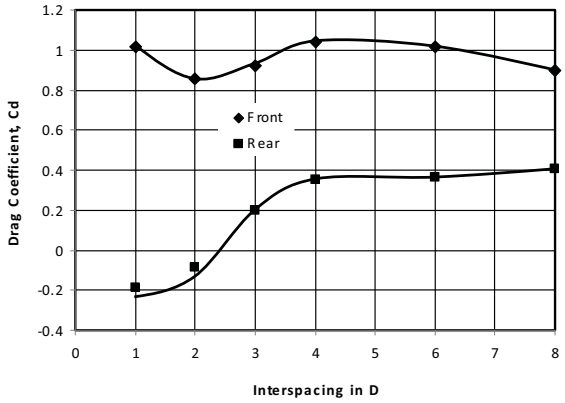

Figure 13: Variation of Drag Coefficient on Front and Rear Cylinders at Different Inter-Spacing

4.0 CONCLUSION

The following conclusions are drawn in regard to the wind effect on the single hexagonal cylinder and the hexagonal cylinders in a group.

a) There is significant drop in the drag coefficient values for the single hexagonal cylinder in comparison to that of the single square cylinder and the values approaches to that of the circular cylinder.

b) The drag coefficient for a single hexagonal cylinder at zero angle of attack is about 0.95 in contrast to that of 2.0 for a single square cylinder at the same angle of attack.

c) The variation of the lift coefficient on the single hexagonal cylinder is not appreciable and they are close to zero value except at angles of attack of 100 and 500, where some insignificant values are observed.

d) The stagnation point is found on the front face of either the single hexagonal cylinder or the front cylinder in the group, however no such stagnation point is found in the rear cylinder of the group.

e) Except at the inter-spacing of 1D, at all other inter-spacing the drag coefficients on the front cylinder of the group are higher than that on the single hexagonal cylinder.

f) There has been remarkable drop in the drag coefficient on the rear cylinder of the group as it falls in the suction region generated by the front cylinder.

g) At some inter-spacing between 2D and 3D, the drag coefficient on the rear cylinder is zero. At the higher inter-spacing the drag coefficients are positive while at the lower inter-spacing they are negative.

h) While wind load is to be used for the design of the free-standing building and group of buildings having hexagonal cross-section, the outcome of the present results may be applied.

REFERENCES

1. Baines W D, "Effects of Velocity Distribution on Wind Loads and Flow Patterns on Buildings", Proceedings of a Symposium on Wind Effects on Buildings and Structures", Teddington, U.K.1963, pp.197-225.

2. Bostock B R and Mair W A, "Pressure Distributions and Forces on Rectangular and D-shaped Cylinders", The Aero-dynamical Quarterly, Vol.23, 1972, pp. 499-511.

3. Castro J P and Fackrell J E, "A Note on Two-Dimensional Fence Flows with Emphasis on Wall Constraint", J. Industrial. Aerodynamics, 3(1), March 1978.

4. Davis R W and Moore E F, "A Numerical Study of Vortex Shedding from Rectangular Cylinder," Journal of Fluid Mechanics, Vol.116, pp.475-506.

5. Hossain M K M, Islam M Q, Mandal A C and Saha S, "Wind Effect on Staggered Cylinders of Square and Rectangular Sections with Variable Longitudinal Spacing", Transaction of the Mech. Eng. Div., The Institution of Engineers, Bangladesh, Vol. ME38, Dec. 2007, pp. 52-57.

6. Hussain H S and Islam O, "Study of wind Load on Buildings and Structures" Journal of the Institution of Engineers, Bangladesh, Vol.1.Nos.2-3, July-October, 1973.

7. Islam A M T and Mandal A C, "Experimental Analysis of Aerodynamic Forces for Cross Flow on Single Rectangular Cylinder", Mechanical Engineering Research Bulletin, BUET, Dhaka, Vol. 13, No. 1, 1990, pp. 36-51.

8. Lawson T V, ''Wind Loadings of Buildings, Possibilities from a Wind Tunnel Investigation," University of Bristol, U. K. Report on TVL/731A, August, 1975.

9. Mandal A C, "A study of Wind Effects on Square Cylinders" M. Sc. Engg. Thesis, Mechanical Engineering Department, BUET, 1979.

10. Mchuri F G et al, "Effects of the free stream Turbulences on Drag Coefficients of Bluff sharp – Edged Cylinders," Nature, Vol.224. No.5222, November 29, 1969, pp. 908-909.

11. M. K. M. Hossain, M. Q. Islam, A. C. Mandal and S. Saha, "Wind effect on staggered cylinders of square and Rectangular sections with variable longitudinal spacings," Journal of Mechanical Engineering, vol. ME38, Dec. 2007, pp-52-57.

12. Parkinson G V and Modi V J, "Recent Research on Wind Effects on Bluff Two Dimensional Bodies," Proceedings, International Research Seminar, Wind Effects on Buildings and Structures, Ottawa, Canada, 1967, pp. 485-514.

13. Surry D, "Pressure Measurements on the Texas Tech Building: Wind Tunnel Measurements and Comparison with Full Scale", J. Wind Eng. Ind. Aerodynamics.no.38, 1991, pp. 235-247.

NOMENCLATURE

Symbol	Meaning
A	Frontal area
C_D	Co-efficient of Drag
C_F	Total force co-efficient
C_L	Co-efficient of Lift
C_P	Mean pressure co-efficient
F_D	Force due to drag
F_L	Force due to lift
Δh_w	Manometer reading
P	Local static pressure
P_O	Free stream static pressure
α	Angle of attack
γ_a	Specific weight of air
γ_w	Specific weight of manometer liquid
ρ	Density of air
ρ_w	Density of water
ΔP	Difference of ambient and local static pressures.
R_e	Reynolds number
U_O	Free stream velocity